Molecular Modeling of H_2 Purification on Na-LSX Zeolite and Experimental Validation

B. Weinberger, F. Darkrim Lamari, S. Beyaz Kayiran, and A. Gicquel
Laboratoire d'Ingénierie des Matériaux et des Hautes Pressions, CNRS UPR1311, 99 Av. J. B. Clément, 93430 Villetaneuse, France

D. Levesque
Laboratoire de Physique Théorique, UMR 8627, Université Paris XI, Bâtiment 210, 91405 Orsay, France

DOI 10.1002/aic.10306
Published online in Wiley InterScience (www.interscience.wiley.com).

Analysis of hydrogen purification process by adsorption in the dehydrated Na-LSX zeolite is described. New measurements of hydrogen and nitrogen adsorption selectivity of this zeolite have been performed up to a pressure of 20 MPa and at temperatures of 273, 293 and 313 K, by using a gravimetric-volumetric method. Structural characterizations were realized by helium density displacement, nuclear magnetic resonance, X-ray diffraction and scanning electronic microscopy. Furthermore, Monte Carlo simulations of gas adsorption were performed in a zeolite model of Na-LSX, using pair potentials to represent the interaction between gas molecules and zeolite atoms. Comparison of simulation results and experimental data enabled testing of the validity of such a modeling of the gas-zeolite interaction. © 2004 American Institute of Chemical Engineers *AIChE J,* 51: 142–148, 2005

Introduction

Hydrogen purification is of increasing interest for future applications in fuel cells (Sircar et al., 1999; Han et al., 2002; Lin et al., 1998; Andrew, 1996). Proton exchange membrane fuel cells need hydrogen of high purity to prevent the degradation of cell membrane efficiency (Baschuk et al., 2001). A major problem lies in producing pure hydrogen at a low price. Now, the cheapest method is that of the natural gas vapor reforming process associated with a purification procedure, so-called pressure swing adsorption (PSA), based on the use of zeolite sieves. These porous materials are already present in several industrial processes, such as selective adsorption, catalysis and ion exchange (Ruthven, 1984; van Bekkum et al., 1991). Adsorption and diffusion of gaseous properties in zeolites are known to be strongly correlated with the nature, amount, and localization of cations in the crystal structure (Darkrim et al., 2000; Porcher et al., 1998). The effects of cations are most readily revealed when zeolites with identical structure differ only in the size, charge, and concentration of exchangeable cations. Studies have been published for Na X zeolite exchanged with divalent cations (Mg, Sr, and so on), where methane adsorption was measured for different exchanged rates at temperatures ranging from 298 to 343 K and at pressures from 1 to 6.9 MPa (Zhang et al., 1991). Kayiran et al. (2002) studied the effect of monovalent cation exchange on the adsorption capacity of LTA zeolites by substituting Li and K cations to Na cations. The measured hydrogen adsorption capacity at high-pressure and ambient temperature varied with the nature of the cations exchanged. Moreover, the barometric study of hydrogen adsorption at 77 K on sodium forms of faujasites with different Si/Al ratios indicates that the number of hydrogen molecules adsorbed per sodium ions is the largest for the Na X zeolite with a Si/Al ratio equal to 1.05 and amounts to one H_2 molecule per sodium cation in the α cages (Kazansky et al., 1998). Adsorption measurements, in beds layered with activated carbon followed by 5A zeolite, for hydrogen separation from a typical cracked gas mixture (H_2/

Correspondence should be addressed to F. D. Lamari at farida.darkrim@limhp.univ-paris13.fr.

$CO_2/CH_4/CO$) have been published (Park et al., 1998). The importance of the selectivity of N_2/H_2 in the purification processes was in particular mentioned by Kohl et al. (1997), Moreau et al. (2002), and Yang et al. (2003). Here, we extend our previous results obtained for hydrogen adsorption in the NaA zeolite (Darkrim et al., 2000) by performing new measurements for the Na-LSX zeolite up to 20 MPa and room-temperature.

In the literature, attempts were made to interpret the experimental results by using numerical simulations of gas adsorption in zeolite models, for instance, xylene (Lachet et al., 1998), residual water (Hutson et al., 2000) and air (Watanabe et al., 1995). In this work, the adsorption properties of a zeolite model are studied by numerical simulations and compared to new experimental data obtained for hydrogen, nitrogen and helium, and for methane, argon and krypton (Vermesse et al. 1996).

In the section "Material Preparation and Characterization", the Na-LSX zeolite used in our experiments is described. In the section "Adsorption Measurements", we present the apparatus used for the material density and gas adsorption measurements. Hydrogen and nitrogen adsorption isotherms are discussed in terms of gas excess adsorption. The section "Molecular Modeling and Discussion" is devoted to a comparison between the experimental results and Monte Carlo simulation data. In the final section, the main conclusions of the study are summarized.

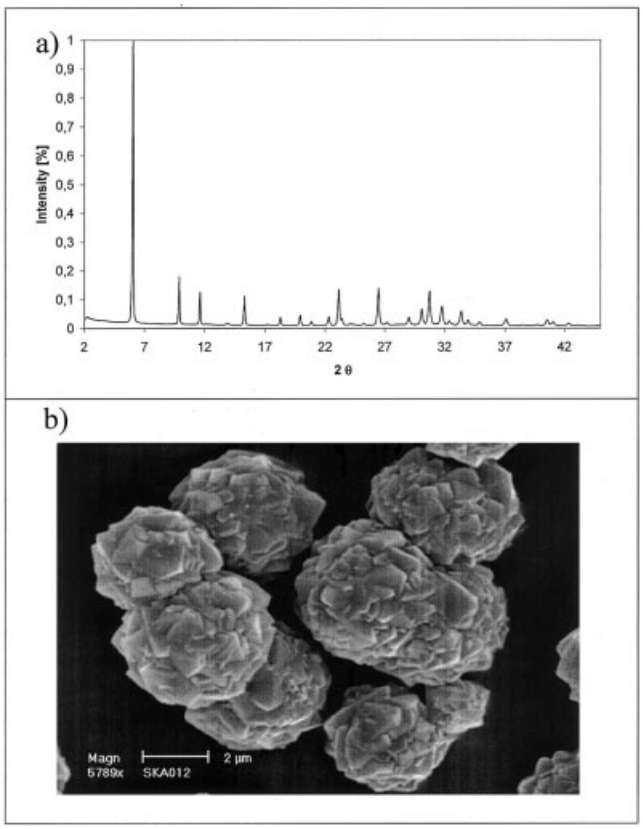

Figure 1. Na-LSX characterizations by (a) X-ray diffraction pattern of the zeolite vs. the diffraction angle, and (b) SEM image of the zeolite sample.

Material preparation and characterizations

Zeolites are microporous materials made of covalently bonded AlO_4 and SiO_4 tetrahedra. They can be prepared with suitably tailored pore dimensions and geometry in order to regulate the penetration and diffusion of the various molecules into the zeolite structure. Zeolites of type A were the first zeolites used for PSA processes (Shen at al., 2001) since 1980, zeolites of type X with an higher selectivity have been introduced in the industrial purification processes. The synthesizing process of LSX zeolite chosen in this work was described by Kühl et al. (1987). The structural characterizations of the zeolite material were made by nuclear magnetic resonance (NMR), X-ray diffraction (XRD) and scanning electronic microscopy (SEM).

NMR experiments were carried out on a Bruker MSL 300 spectrometer using a standard CP/MAS probe 7 mm rotor, operating at a frequency of 59.63 MHz. The rotor spun at 4 kHz, pulse was spaced of 100 s (flip angle of 45°), and the radio frequency field was 55.5 kHz. The X-ray powder diffraction patterns of our zeolite sample were collected with a STOE STADI P diffractometer using (Kα1) Cu radiation, and the SEM pictures on a Philips XL30 apparatus. The ^{29}Si MAS NMR spectrum displayed a unique peak located at 84.22 ppm typical of an ordered X-type zeolite with an Si/Al ratio equal to 1, and a strict alternation of Si and Al on the framework sites (Klinowski, 1984). ^{27}Al MAS NMR spectroscopy showed a single band at 58.4 ppm, consistent with Al tetrahedral framework. There is a full agreement between ^{29}Si and ^{27}Al MAS NMR measurements. Figure 1a shows the X-ray diffractogram of the zeolite LSX. The sample was fully crystallized, without the presence of impurities and colloids. This conclusion was reached by reference to a standard pure LSX zeolite diffraction pattern, which enables the verification of the absence of impurity peaks on the diffractogram. The SEM image confirmed that our sample was well-crystallized (Figure 1b).

Adsorption measurements

The main adsorption measurement procedures are the volumetric method (Kiyobayashi et al., 2002; Berlier et al., 1995; Vidal et al., 1990; Dollimore, 1973) and gravimetric method (Dreisbach et al., 2002; De Weireled et al., 1999). The measurement of the hydrogen adsorption isotherms presents specific problems induced by the weak bulk density of this gas. To obtain reliable results, we used the absolute gravimetric-volumetric method, which is especially convenient for measurement of high-pressure adsorption isotherms (Figure 2a). The adsorption excess m_a can be computed from the following mass balance formula $m_a = m_G - [V_C - (m_{Ads}/\rho_{Ads})]\rho_G$ where m_{Ads} and m_G are the adsorbent and adsorbed gas masses, respectively. ρ_{Ads} is the adsorbent density, such as it is defined in Lowel et al., 1984. V_c is the cell volume which takes into account the dilatation effects, and ρ_G is the bulk gas density at the experimental conditions obtained from Gas Encyclopaedia Tables (1976).

The reactor was filled with the adsorbent and out-gassed, while the temperature was increased steadily by 2 K per min up to 373 K. This temperature was maintained until the final pressure of 10^{-4} Pa was reached. The aim of this procedure

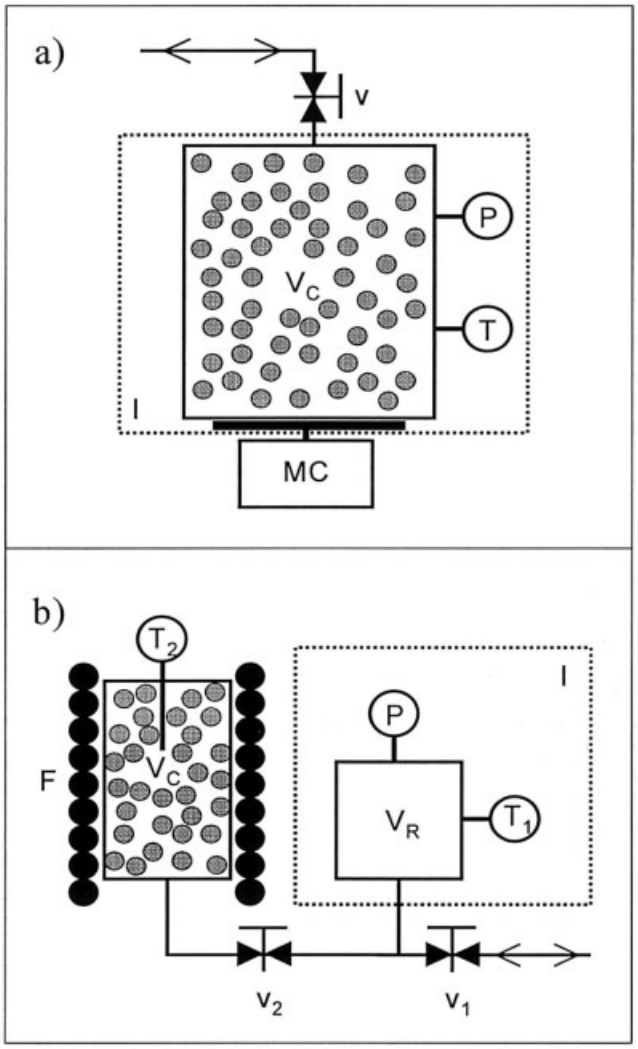

Figure 2. (a) Measuring device of gas adsorption at high pressure: v valve, V_C measurement cell, MC mass comparator (Mettler PR2004), P digital quartz manometers (DH Budenberg DPM1, Heise 901B), T platinum resistance thermometer, I incubator (France Etuves), and (b) the measuring device for the determination of Helium density: F furnace, T_1, T_2 platinum resistance thermometers, V_C measurement cell, P quartz digital manometer (Paroscientific 710), V_R reservoir volume, I incubator (S.P.A.M.E.), v_1, v_2 valves.

was to ensure full dehydration without damaging the adsorbent. In order to eliminate adsorbed gases, the adsorbent was heated using a ramp of 2 K per min, between 573 K and 673 K, depending on the adsorbent nature. When the final pressure of 10^{-4} Pa was reached (48h) the reactor was cooled down to room-temperature and weighed with the mass comparator (PR2004). The gas (99.9996% for hydrogen and 99.9995% for nitrogen) was injected into the cell, containing the out-gassed solid, which was linked to the mass comparator. The temperature in the incubator was regulated between 273 and 333 K, with a precision of ± 0.1 K. For each measurement point, pressure was monitored until equilibrium. At the latter pressure, the excess adsorbed amount was calculated from the total adsorbed mass (Table 1). The pressure measurements were made below 6.9 MPa with DH Budenberg DPM1, and up to 70 MPa with the high-pressure Heise 901B manometer (p_{max} = 200 MPa). The use of a primary digital quartz manometer was necessary to achieve, at low-pressures, an acceptable accuracy in results. Pressures higher than 20 MPa and up to 70 MPa was obtained by using a gas compressor (Schmidt, Kranz & Co. GmbH). With the above described experimental apparatus and procedure, the problem of the leak detection was solved by controlling the stability of the experimental cell weight. Our measurement of the adsorbent density was based on the helium displacement method. Initially, the adsorbent was regenerated following a procedure similar to that described above for adsorption measurements and weighed (Figure 2b). Helium gas (99.9996%) was injected into the reservoir cell. After pressure and temperature stabilization, the gas density was evaluated using the IUPAC tables (Angus et al., 1977). Upon opening the valve v_2, the helium penetrated into the dead space of the measurement cell, heated up to 650 K. In order to rule out the possibility of a slow diffusion, the pressure was observed for over 1 h. The adsorbent density ρ_{Ads} is obtained from $\rho_{Ads} = [m_{Ads}\rho_2/\rho_2 V_C - V_R(\rho_0 - \rho_1)]$ where m_{Ads} is the absorbent mass and ρ_0 the helium gas density before expansion. ρ_1 and ρ_2 represent helium densities after expansion in the reservoir and the measurement cell, respectively. The volumes of the reser-

Table 1. Experimental Adsorptions of Nitrogen and Hydrogen on Na-LSX Zeolite at 293, 313 and 333 K

p [MPa]	$1/v$ [10^3 mol/m^3]	m_a [mol/kg]
	293 K − N_2	
0.5132	0.2108	1.28
1.0013	0.4116	1.95
1.9550	0.8048	2.57
2.9891	1.2319	2.89
4.0103	1.6535	3.11
5.0209	2.070	3.26
	313 K − N_2	
0.5079	0.1951	0.92
1.0257	0.3942	1.49
1.9953	0.7669	2.12
3.0567	1.1744	2.49
4.0076	1.5386	2.69
5.0259	1.9271	2.86
	333 K − N_2	
0.4981	0.1798	0.66
1.0103	0.3645	1.17
2.0038	0.7223	1.72
3.0105	1.0838	2.05
3.9815	1.4312	2.27
5.0130	1.7984	2.43
	293 K − H_2	
0.8742	0.3567	0.13
1.8721	0.7595	0.26
2.7519	1.1107	0.36
3.5896	1.4416	0.45
4.6265	1.8767	0.56
5.6523	2.2426	0.65
7.6620	3.0039	0.84
10.283	3.9696	0.99
12.637	4.8110	1.09
14.973	5.6226	1.18
17.491	6.4721	1.25
19.121	7.0085	1.30

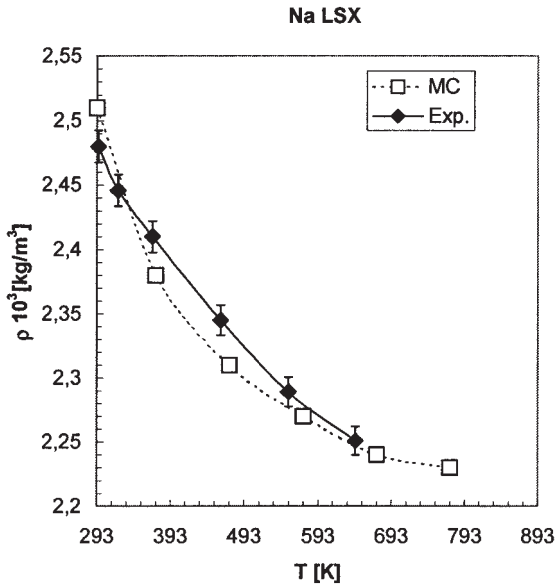

Figure 3. Measurements and Monte Carlo simulations for Helium density of the zeolite Na-LSX at different temperatures.

voir and measurement cell were previously calibrated using xenon as standard gas, with accuracy better than 0.1%. We measured the Na-LSX density at different temperatures. The density decreased with the increase in temperature (see Figure 3). Similar results were found by Malbrunot et al. (1997) and Dreisbach et al. (2002). The adsorbent density becomes weakly dependent on the temperature above 500 K. Therefore, it seemed justified to choose ρ_{Ads} equal to 2.25 10^3 kg/m^3 for calculating gas excess adsorption.

Molecular modeling and discussion

The experimental measurements of gas adsorption described in this work, along with results of previous experiments (Vermesse et al., 1996), constitute a set of data which seem adequate for attempting to quantitatively estimate the validity of the interaction modeling the interaction modeling between gases and the Na-LSX zeolite. Thus, Grand Canonical Monte-Carlo (GCMC) simulations are a theoretical tool used in numerous works on adsorption in zeolites (Vlugt et al., 1998; Smit et al., 2001; Watanabe et al., 1995, Smit et al., 1994). The realization of such GCMC simulations requires a knowledge of the atom positions in the zeolite crystal, and a detailed description of interactions between the adsorbed atoms or molecules and zeolite atoms. For the Na-LSX zeolite considered in this work, an accurate localization of atom positions is available in the literature. The Na-LSX zeolite has a unit cell of side 2.51 nm, and the stochiometric formula is Al_{96} Si_{96} O_{384} Na_{96}. The atomic positions given, for instance, in Porcher (1998), are in good agreement with those of Lee et al. (1998). A plot of the Na-LSX unit cell used in GCMC simulations is shown in Figure 4. Some simplifications compared to X-ray diffraction data have been introduced. The main simplification concerns the distances between Al and Si nearest neighbors chosen equal to 0.3139 nm irrespective of the localization of these atom pairs in the crystal. Thus, the faces of sodalite units are strictly hexagonal or square. Consequently, the distances between O atoms and nearest neighbor Al and Si atoms are equal to 0.1730 nm and 0.1621 nm, respectively. There are different possible localization sites for Na cations. We have chosen those given by Porcher (1998). Eight cations are localized near the center of the hexagonal faces on the sites referred to as I' and II in the literature. Four cations are close to square faces of sodalite units and external faces of hexagonal prisms inside the cages α (referred to as IIIa and IIIb).

Interactions between the atoms or molecules of adsorbed gases are described by pair potentials, assuming that each zeolite atom is the source of van der Waals and coulomb potentials. In the literature, the van der Waals potentials of the zeolite atoms (Watanabe et al. 1995; Smit et al., 1994; Vlugt et al., 2002), and those of atoms or molecules of simple gases are often represented by Lennard-Jones (LJ) potentials

$$v(r) = 4\varepsilon\left(\left(\frac{\sigma}{r}\right)^{12} - \left(\frac{\sigma}{r}\right)^{6}\right)$$

and the crossed interactions between zeolite, and gases are obtained from the Lorentz-Berthelot's rule (cf. Darkrim et al., 2000). The ε parameters can be approximately obtained by using the London formula or similar expressions (Hirschfelder et al., 1954; Dzhigit et al., 1979; Hansen et al., 1986). The effective charges of zeolite atoms can be calculated from theoretical approaches (Mortier et al., 1986; Van Genechten et al. 1988; Henry, 1994). Electric multipoles of hydrogen and nitrogen molecules are described by a linear electric quadrupole corresponding to a distribution of three effective charges given in Table 2. The LJ parameters for gas atoms or molecules: He, Ar, Kr, H_2, N_2 and CH_4 are taken as equal to ε =10.2, 119.8, 164.4, 36.7, 36.4 and 148.2 K and σ = 0.2556, 0.3405, 0.3684, 0.2958, 0.3318, and 0.3817 nm, respectively. These LJ potentials are located at the center of mass of atoms or molecules except for N_2 molecules, where two LJ potentials were centered to the positions of N atoms. Table 3 presents the LJ parameters and effective charges associated to the zeolite atoms. The GCMC simulations of gas adsorption were performed for a crystal of the Na-LSX zeolite of eight unit cells

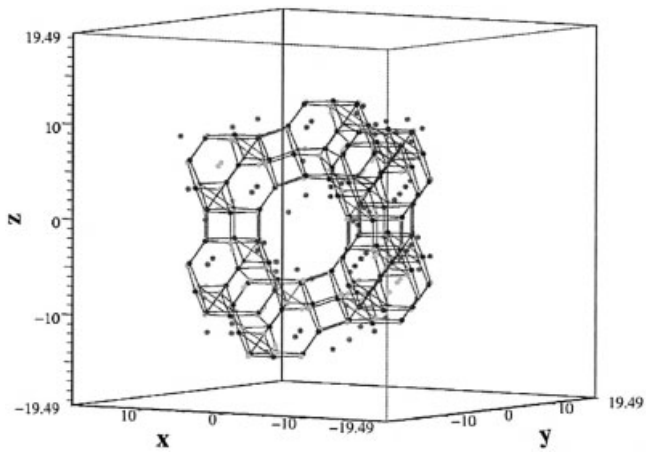

Figure 4. Na-LSX cell used in the GCMC simulations.

The isolated dots indicate the positions of Na cations. The lines link Si-Al nearest neighbors.

Table 2. Coulombic Potential Parameters for the Adsorbed Gases

Gas	Q	α	q	$d/2$
He	0	0.206	—	—
Ar	0	1.64	—	—
Kr	0	2.48	—	—
H_2	0.637	0.8	0.21	0.037
N_2	−1.4	1.7	0.20	0.055
CH_4	0	2.60	—	—

Column 1 gives the gas. Column 2 corresponds to the quadrupole (10^{-26} esu) of the gases. (α) is the polarizability (10^{-30} m^3) of the gases. (q) is the charge (ues) associated to the gas molecule quadrupole. ($d/2$) is the distance (nm) between the charges in the molecule.

located in a parallelepipedic volume V_C equal to 125.567 nm^3 of sides $L_x = 3.5344$ nm, $L_y = 6.152$ nm, and $L_z = 5.7749$ nm with periodic boundary conditions. The size of the zeolite crystal was chosen so that the upper boundary of the interatomic distance used to compute the van der Waals interactions was on the order of 1.5 nm. The long range of the coulombic interactions was taken into account by using of the Ewald summation method (De Leeuw et al., 1980; Frenkel and Smit "Understanding Molecular Simulation", 1996). We took into account the interaction between effective charges and polarizability of adsorbed molecules. The polarization effects were computed at the first-order in the polarization α_g of gas atoms or molecules; the contribution E_P of these effects to gas-zeolite interaction energy is given by

$$E_P = -\frac{1}{2}\sum_{i=1,N} \alpha_g \vec{E}(r_i)^2$$

where $\vec{E}(r_i)$,, is the electric field due to zeolite charges at position r_i of the center of mass of gas atoms or molecules. In simulations, we used a set of effective charges identical to that considered in those made in the reference Darkrim et al. (2000), for H_2 adsorption in the NaA zeolite, with the exception of the effective charges of Na cations localized inside cages α. Such a choice seems acceptable since the structural arrangement of atoms constituting sodalite units does not differ greatly between NaA and Na-LSX zeolites. Since the localization of Na cations inside α cages is different between NaA and Na-LSX zeolites, the effective charge of Na cations localized in positions IIIa and IIIb was chosen as being equal to 0.8 e (e electron electric charge). The comparison of the experimental results for the excess adsorption with simulation data needed to determine the volume occupied by the zeolite atom in the simulation cell. This latter volume was estimated similarly to helium displacement procedure (Malbrunot et al. 1997), by

Table 3. Parameters of Coulombic and Lennard-Jones Potentials for Na-LSX Zeolite

Atom	ε	σ	q
Al	19.01	0.101	1.4
O	42.	0.2708	0.6
Na	8.0	0.35	0.8
Si	18.1	0.0677	0.8

Column 1 gives the atom of the zeolite. (ε) and (σ) are the Lennard-Jones potential parameters (K) and (nm). (q) corresponds to the charge associated to zeolite atom (ues).

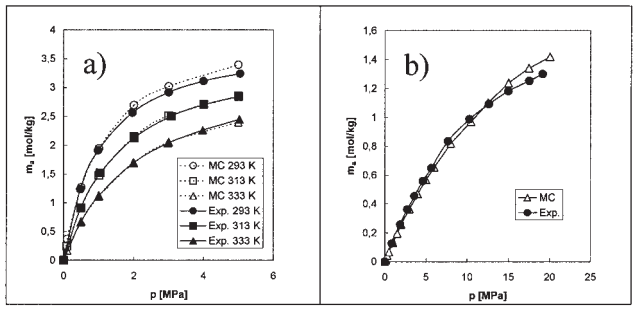

Figure 5. Measurements and Monte Carlo simulations of the excess adsorption for (a) nitrogen at 293, 313 and 333 K between 0 and 5 MPa; (b) hydrogen at 293K between 0 and 20 MPa on Na LSX zeolite.

computing in the Na-LSX zeolite model, the adsorption of He. The bulk density ρ_s of the adsorbent is given by $\rho_S = m_z/(V_c - \langle N_{He}\rangle/\rho^b_{He})$ where m_z is the zeolite mass, $\langle N_{He}\rangle$ is the computed average number of He atoms in the simulation cell and ρ^b_{He} is the bulk density of He at the pressures and temperatures of the simulations. Excellent agreement was obtained between ρ_{Ads} and ρ_s values (Figure 3). The variation in ρ_s with temperature indicates that the hypothesis of a weak contribution of He-zeolite interactions to adsorption seems valid for temperature above 500 K. The obtained value $\rho_s = 2.25\ 10^3$ kg/m^3 at high-temperature is compatible with crystallographic data (Breck 1974; Goulay et al. 1996). Excess adsorption, for the considered gases, is obtained from simulation data by the relation $\rho_{ex} = (N_{sim} - V_a\rho^b)/N_{av}m_Z$ where N_{sim} is the average number of gas atom or molecules, present in the simulation cell, computed for a given pressure and temperature, and ρ^b is the bulk density of gases at the same thermodynamic state. N_{av} is the Avogadro number. The values of ρ^b are computed from the equation of state of systems interacting by LJ potentials (Johnson et al. 1993). For N_2 and H_2, the contributions of quadrupolar interactions to the equation of state are small below 150 MPa at room-temperature. The agreement of the LJ equation of state with the equations of state of the considered gases at room-temperature and high-pressure can be checked by comparison with the data basis of the National Institute of Standards and Technology (2003). N_{sim} was computed with an accuracy of ~1 to 2% from a sampling of ~8 10^6 configurations realized for each thermodynamic state.

The choice of LJ parameters and effective charges enables to reaching excellent agreement between the N_2 experiment and simulation data for the 3 excess adsorption isotherms at moderate pressures (Figure 5). At higher pressure and 298 K, the agreement remains favorable, since the difference $N_{sim} - V_a\rho^b$ becomes slight compared to N_{sim} (Figure 6c). For pressures above 100 MPa, simulation-experiment agreement is more difficult to achieve, since a difference of ~ 20% between theoretical and measured excess adsorption corresponds to, only ~ 1% of the total adsorption. Indeed, good agreement between simulation and experiment for argon, krypton and methane gases is obtained at high pressure, since the differences of ~10–30% between the two sets of data can be interpreted on the same basis as those found in the case of N_2 (Figure 6a, 6b and 6d). The proposed force field of Na-LSX

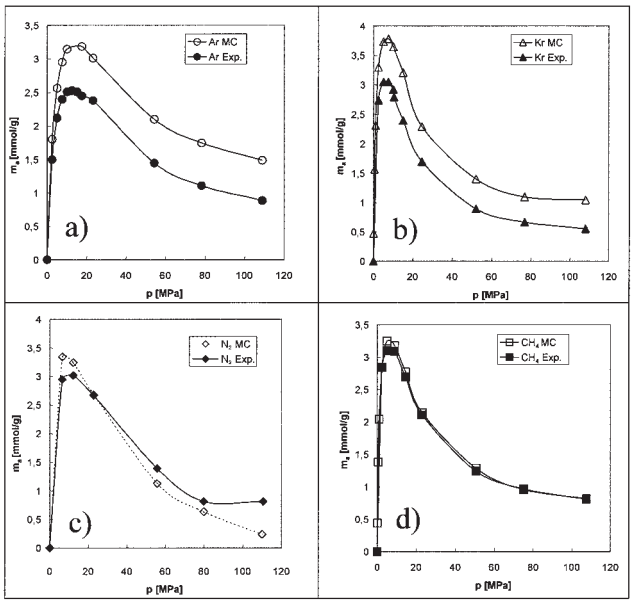

Figure 6. Measurements (Vermesse et al., 1996) and Monte Carlo simulations of excess adsorption for Na-LSX zeolite at high-pressure and room-temperature for (a) argon, (b) krypton, (c) nitrogen, and (d) methane.

zeolite gives a good, almost quantitative description of the adsorption of He, N_2, CH_4, Ar and Kr in a large domain of pressures. This result is obtained by supposing that the properties of the gas atoms or molecules are identical in the bulk and adsorbed phases (cf. LJ parameters given above and Table 2). With this hypothesis the selectivity N_2/H_2 at 1 MPa and 293K is predicted by simulation equal to 8-9 compared to the value of ~13, found experimentally. Since the validity of the force field seems established by the agreement obtained for five simple gases, the weak adsorption of H_2 corresponding to the very high selectivity N_2/H_2 has been preferentially interpreted by an alteration of the properties of H_2 molecules in the adsorbed phase. A good agreement, in particular below 10 MPa, is found between experimental and simulation data with an effective polarizability of 0.36 10^{-30} m^3 (cf. Figure 5). Clearly, this hypothesis of a variation of H_2 bulk properties in the confined environment of zeolite α cages certainly needs a more detailed investigation, for instance, on the basis of *ab initio* computations (Banerjee et al., 2002; Arbuznikov et al. 1998; Anderson et al. 1999; MacKinnon et al. 2001).

Conclusion

Accurate measurements of adsorption of N_2 and H_2 were performed up to pressures of 20 MPa on a zeolite sample. This zeolite has been shown to present all the characteristics of pure and homogeneous Na-LSX zeolite crystals according to the NMR, XRD and SEM characterization procedures. Using the helium displacement method, material density and accessible volume for the gas molecules were estimated, enabling determination of the excess adsorption of N_2 and H_2 on an unambiguous basis since, between 550 and 650 K, the adsorbent density value varied by less than 1.5%. The experimental N_2/H_2 selectivity at room-temperature and 1 MPa was equal to ~13. This result suggests to an excellent selectivity of the Na-LSX zeolite between H_2 and N_2. The Na-LSX zeolite model is able to predict almost quantitatively the excess adsorption of simple gases (He, N_2, Ar, Kr and CH_4) over a large range of pressures when the contribution of the molecular polarizability at the gas-zeolite interaction is taken into account.

The main conclusion of this article is that, on the basis of our experimental data and numerical prediction, the Na-LSX zeolite is an excellent material to separate hydrogen gas from nitrogen which would be present in hydrogen production units.

Acknowledgment

The authors thank Air Liquide for a financial grant and Dr. S. Moreau for many interesting scientific discussions. Also, we thank M. Bono and M. Beauverger for their permanent technical support.

Literature Cited

Anderson, C.-R., D. F. Cocker, J. Eckert, and A. L. R. Bug "Computational Study of Molecular Hydrogen in Zeolite Na-A. I. Potential Energy Surfaces and Thermodynamic Separation Factors for *Ortho* and *Para* Hydrogen," *J. Chem. Phys*., **111**, 7599 (1999).

Andrew L. D., "Hydrogen Generation from Natural Gas for the Fuel Cell Systems of Tomorrow," *J. Power Sources*, **61**, 113 (1996).

Angus, S., and K. M. de Reuck, *IUPAC Helium International Tables of Fluid State-4*, Pergamon Press, London (1977).

Arbuznikov, A., V. Vasilyev, and A. Goursot., "Relationships Between the Structure of a Zeolite and its Adsorption Properties," *Surface Sci.*, **397**, 395 (1998).

Banerjee A., K. D. Sen., J. Garza, and R. Vargas, "Mean Excitation Energy, Static Polarizability, and Hyperpolarizability of the Spherically Confined Hydrogen Atom," *J. Chem. Phys*., **116**, 4054 (2002).

Baschuk J. J., and X. Li., "Carbon Monoxide Poisoning of Proton Exchange Membrane Fuel Cells," *Int. J. Energy Res.*, **25**, 695 (2001).

Berlier K, J. Bougard, and M-G. Olivier, "Automatic Measurement of Isotherms of Adsorption on Micro Porous Media in Large Ranges of Pressure and Temperature," *Meas. Sci. Technol.,* **6**, 107 (1995).

Breck D. W., *Zeolite Molecular Sieves*, Krieger Publishing Co., Malbar, FL (1974).

Darkrim F., P. Malbrunot., A. Aoufi., and D. Levesque, "Hydrogen Adsorption in the NaA Zeolite: A Comparison Between Numerical Simulations and Experiments," *J. Chem. Phys*., **112**, 5991 (2000).

De Leeuw S. W., J. W. Perram., and E. R. Smith, "Simulation of Electrostatic Systems in Periodic Boundary Conditions. I. Lattice Sums and Dielectric Constants," *Proc. R.. Soc. London*, **373**, 26 (1980).

De Weireld G., M. Frère, and R. Jadot, "Automated Determination of High-Temperature und High-Pressure Gas Adsorption Isotherms using a Magnetic Suspense Balance," *Meas. Sci. Technol.,* **10**, 117 (1999).

Dollimore D., G. R. Rickett Robinson, "The Design and Operation of a Simple Volumetric Adsorption Apparatus," *J. Phys. E*, **6**, 94 (1973).

Dreisbach, F., H. W. Lösch., P. Harting, "Highest Pressure Adsorption Equilibria Data: Measurement with Magnetic Suspension Balance and Analysis with a New Adsorbent/Adsorbate Volume," *Adsorption*, **8**, 95 (2002).

Dzhigit, O. M., A. V. Kiselev., T. A. Rachmanova, and S. P. Zhdanov,"Influence of Li^+, Na^+ and K^+ cation Concentrations in X and Y Zeolites on Isotherms and Heat of Adsorption of Propane and Water," *J. Chem. Soc. Farady Trans.* 1, **75**, 2662 (1979).

Frenkel, D., and B. Smit, *Understanding Molecular Simulation: From Algorithms to Applications*, Computational Science Series, Academic Press, New York (1996).

Gas Encyclopedia, L'Air Liquide Division Scientifique, Elsevier (1976).

Goulay A. M., J. Tsakiris, and E. Cohen de Lara, "Molecular Interactions in Nanoporous Adsorbents. Adsorption of N_2 and O_2 in Zeolites with Cavities or Channels: $Na_{12}A$, Ca_6A, NaX, and Decationated Mordenite," *Langmuir*, **12**, 371 (1996).

Han J., Kim I.-S., Choi Keun-Seob, "High Purity Hydrogen Generator for on-site Hydrogen Production," *I. J. Hydrogen Energy*, **27**, 1043(2002).

Hansen, J. P., and I. R. McDonald, *Theory of Simple Liquids*, Academic Press, New York (1986).
Henry M., "Partial Charge Distributions in Crystalline Materials through Electronegativity Equalization," *Mater. Sci. Forum,* **152**, 355 (1994).
Hirschfelder, J. O., C. F. Curtiss, and B. R. Bird, *Molecular Theory of Gases and Liquids*, Wiley, New York (1954).
Hutson, N.D., Zajic S. C., andYang R. T., "Influence of Residual Water on the Adsorption of Atmospheric Gases in Li-X zeolite : Experiment and Simulation," *Ind. Eng. Chem. Res.*, **39**, 1775 (2000).
Johnson, J. K., J. A. Zollweg, and K. E. Gubbins,"The Lennard-Jones Equation of State Revisited," *Mol. Phys*., **78**, 591 (1993).
Kayiran, S., F. Lamari Darkrim, and A. Gicquel, "Synthesis and Ionic Exchanges of Zeolites for Gas Adsorption," *Surface and Interface Analysis*, **34**, 100 (2002).
Kazansky, V. B., V. Yu. Borovkov, A. Serich., and H. G. Karge, "Low Temperature Hydrogen Adsorption on Sodium Forms of Faujasites: Barometric Measurements and Drift Spectra," *Microporous and Mesoporous Mat.*, **22**, 251 (1998).
Klinowski, "Nuclear Magnetic Resonance Studies of Zeolites," *Progress in NMR Spectroscopy*, **16**, 237 (1984).
Kiyobayashi, T., H. T Takeshita, H. Tanaka., N. Takeichi., A. Züttel., L. Schlapbach, and N. Kuriyama, "Hydrogen Adsorption in Carbonaceous Materials : How to Determine the Storage Capacity Accurately," *J. of Alloys and Compounds*, **330**, 666 (2002).
Kohl, A., and R. Nielsen, *Gas Purification*, Gulf Publishing Company, Houston (1997)
Kühl, G. H., "Crystallization of Low-Silica faujasite ($SiO_2/Al_2O_3 \sim 2.0$)," *Zeolites*, **7**, 451 (1987)
Lachet, V., A. Boutin, B. Tavitian, A. H. et Fuchs, "Computational Study of p-xylene/m-xylene Mixtures Adsorbed in NaY Zeolite," *J. Phys. Chem. B.*, **102,** 9224 (1998).
Lee, Y., S. W. Carr, and J. B. Parise, "Phase Transition upon K^+ Ion Exchange into Na-Low Silica X: Combined NMR and Synchrotron X-ray Powder Diffraction Study," *A. Chem. Soc*., **10**, 2561(1998).
Lin, Y.-M., G.-L, Lee, and M.-H. Rei, "An Integrated Purification and Production of Hydrogen with a Palladium," *Catalysis Today*, **44**, 343 (1998).
Lowell, S., and J. E. Shields, *Powder Surface Area and Porosity*, Chapman and Hall, New York (1984).
MacKinnon, J. A., J. Eckert, D. F. Coker, and A. L. R. Bug, "Computational Study of Molecular Hydrogen in Zeolite Na-A. II. Density of Rotational States and Inelastic Neutron Scattering Spectra," *J. Chem. Phys.,* **114**, 10137 (2001).
Malbrunot, P., D, Vidal., Vermesse J., Chahine R., and T. K. Bose, "Adsorbent Helium Density Measurement and Its Effect on Adsorption Isotherms at High Pressure," *Langmuir*, **13**, 539 (1997).
Moreau, S., and B. Polster,"Process for the Production of Hydrogen Using a Carbonated Adsorbent with Selected Dubinin Parameters," *L'Air Liquide*, U.S. Patent 6,**425**,939 (2002).
Mortier, W. J., S. K. Ghosh., and S. Shankar., "Electronegativity-Equalization Method for the Calculation of Atomic Charges in Molecules," *J. Am. Chem. Soc*., **108**, 4315 (1986).
National Institute of Standards and Technology, "NIST Thermodynamic and Transport Properties of Pure Fluids Database: Version 5.0," NIST, Gaithersburg, MD (2003).
Park, J.-H., J.-N. S.-H. Kim Cho, J.-D. Kim, and R. T. Yang, "Adsorber Dynamics and Optimal Design of Layered Beds for Multicomponent Gas Adsorption," *Chem. Eng. Sci*., **53**, 3951 (1998).
Porcher, F., "Cristallographie Très haute RéSolution et Propriétés éIectrostatiques de Monocristaux de Zéolithes A et X déshydratés," Thèse, Université Henri Poincaré, Science des Matériaux, Nancy I (1998).
Porcher, F., M. Souhassou, Y. Dusausoy, and C. Lecomte, "Structure Cristalline sur Monocristal de la Zéolithe LiA Totalement échangée et déshydratée," *Comptes Rendus de l'Académie des Sciences -Serie II-C-Chimie*, **1**, 701, (1998).
Ruthven, D. M., *Principles of Adsorption and Adsorption Processes*, Wiley, New York (1984).
Shen, D., M. Bülow., S. R. Jale., F. R Fitch., and A. F. Ojo., "Thermodynamics of Nitrogen and Oxygen Sorption an Zeolites Li-LSX and Ca-A," *Mic. and Mes. Mat*., **48**, 211 (2001).
Sircar, S., W. E. Waldron, M. B. Rao, and M. Anand, "Hydrogen Production by Hybrid SMR-PSA-SSF Membrane System," *Sep. Purif. Technol.*, **17**, 11 (1999).
Smit, B., and R. Krishna, "Monte Carlo Simulations in Zeolites,"*Curr. Opin. Solid. St. M*., **5**, 455 (2001).
Smit, B., and J. I. Siepmann, "Computer Simulations of the Energetics and Siting of n-Alkanes in Zeolites", *J. Phys. Chem.*, **98**, 8442 (1994).
van Bekkum, H., E. M. Flanigen, and J. C. Jansen, *Introduction to Zeolite Science and Practice,* Elsevier, Amsterdam (1991).
van Genechten, K. A., and W. J. Mortier, "Influence of the Structure Type on the Intrinsic Framework Electronegativity and the Charge Distribution in Zeolites with SiO_2 Composition, " *Zeolites*, **8**, 273 (1988).
Vermesse, J., D. Vidal, and P. Malbrunot, "Gas Adsorption on Zeolites at High Pressure," *Langmuir*, **12**, 4190 (1996).
Vidal, D., Malbrunot P., Guengant L. and Vermesse J., "Measurement of Physical Adsorption of Gases at High Pressure," *Rev. of Scientific Instruments*, **61**, 1314 (1990).
Vlugt, T. J. H., W. Zhu., F. Kapteijn, J. A. Moulijn, B. Smit., R. Krishna, "Adsorption of Linear and Branched Alkanes in the Zeolite Silicalite-1," *J. Am. Chem. Soc*., **120**, 5599 (1998).
Watanabe, K., N. Austin., and M. R. Stapleton, "Investigation of the Air Separation Property's of Zeolites Type A,X and Y by Monte Carlo Simulation," *Molecular Simulation*, **15**, 197 (1995).
Yang, R. T., *Adsorbents: Fundamentals and Applications*, Wiley, Hoboken, NJ (2003).
Zhang, S. Y., O. Talu., and D. T. Hayhurst, "High Pressure Adsorption of Methane in Na-LSX, MgX, CaX, SrX and BaX," *J. Phys. Chem.*, **95**, 1722 (1991).

Manuscript received Oct. 13, 2003, and revision received Apr. 27, 2004.